Prostate Brachytherapy Seed Segmentation Using Spoke Transform

Steve T. Lam[a], Robert J. Marks II[a] and Paul S. Cho[a.b]

[a]Dept. of Electrical Engineering, Univ. of Washington
Seattle, WA 98195-2500 USA

[b]Dept. of Oncology, Univ. of Washington
Seattle, WA 98195-6043 USA

ABSTRACT

Permanent implantation of radioactive seeds is a viable and effective therapeutic option widely used today for early stage prostate cancer. In order to perform intraoperative dosimetry the seed locations must be determined accurately with high efficiency. However, the task of seed segmentation is often hampered by the wide range of signal-to-noise ratios represented in the x-ray images due to highly non-uniform background. To circumvent the problem we have developed a new method, the *spoke transform*, to segment the seeds from the background. This method uses spoke-like rotating line segments within the two concentric windows. The mean intensity value of the pixels that fall on each rotated line segment best describing the intersection between the seed that we are trying to segment is chosen. The inner window gives an indication of the background level immediately surrounding the seeds. The outer window is an isolated region not being segmented and represents a non-seed area in need of enhancement and a detection decision. The advantages of the method are its ability (1) to work with spatially varying local backgrounds and (2) to segment the hidden seeds. Pd-103 and I-125 images demonstrate the effectiveness of the spoke transform.

Keywords: image segmentation, seed segmentation, medical image processing, signal processing

1.   INTRODUCTION

In the past decade, the reported incidence of prostate cancer has grown dramatically. This increase is believed to be primarily due to longer life expectancy, awareness of prostate cancer and enhanced techniques in screening and diagnostic procedures[6]. Therefore, the number of patients seeking medical care for prostate diseases is also increased steadily. One of the current treatments for early-stage prostate carcinoma, that is widely recognized, is the implantation of radioactive seeds in the prostate. The x-ray is a valuable tool in analyzing dose distribution. The seed image acquisition is the projection of x-rays captured with fluoroscopy or film. In order to perform the dose distribution analysis, seed locations must be determined by segmenting the seeds. The difficulty of segmenting the seeds in x-ray images is that the resulting images may have very low signal to noise ratios and the seeds spread over various background structures with non-uniform brightness. In addition, some seed images are difficult to identify with the naked eye due to the extremely low contrast with respect to the background. Some of the new clustering approaches such as active contour models, fuzzy clustering, neural networks, Markov random field models, etc. have been used to solve the problem of segmentation[8-10]. While there have been various approaches proposed for medical image segmentation[1-5], many processing techniques can be used to segment but with various success – especially when applying these methods to segment the seeds in prostate x-ray images.

In this paper, we propose a new method, the spoke transform, to segment the seeds from the background. By incorporating the seed's surrounding regions, the spoke transform can effectively utilize

and compare the seeds and surrounding regions to segment the seeds. Successful application of our method to segment the seeds from the real world images is presented.

2.   MATERIAL AND METHODS

Standard edge detection algorithms applied to segment seeds will result in many faulty edges[7]. This is because the signal to noise ratios between the seeds and various backgrounds are very low. Conventional segmentation algorithms use image gradients and fail to accurately detect the seeds where the contrast is poor. Kernel windows of different size must be used for different backgrounds and seed types. The spoke transform utilizes the contrast between the seeds and the adjacent surrounding backgrounds to segment the seeds. The enhanced image generated by the spoke transform is then thresholded to give the segmented seeds. The spoke transform algorithm is illustrated the flow chart in Fig. 1.
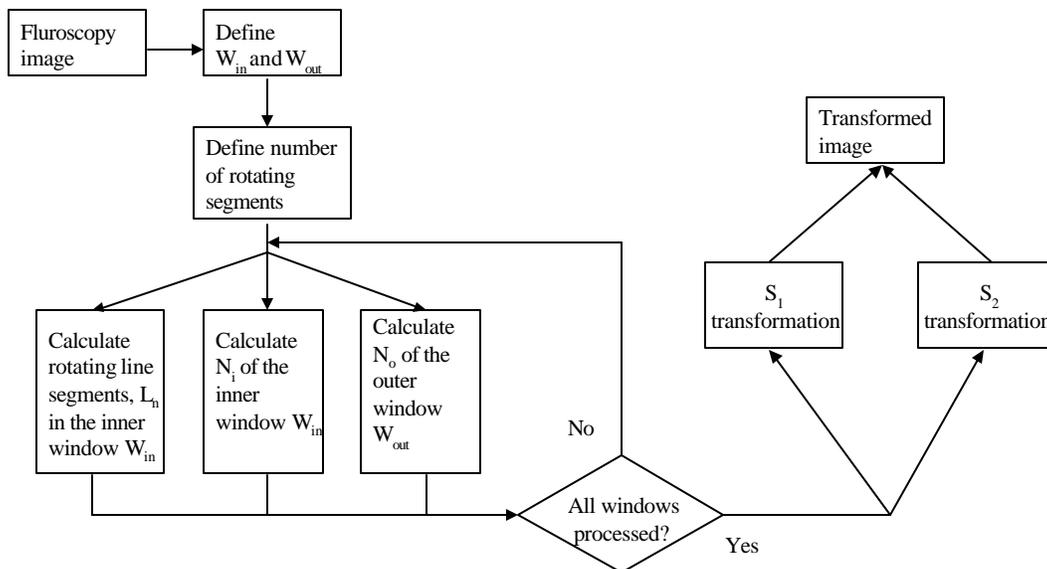
Figure 1: Spoke transform

3.   DEFINING SPOKES

For an $(L_x \times L_y)$ image with intensity pixel values, I, the spokes are defined by the relationship between a set of pixels of two concentric windows, the inner window W_{in} and the outer enclosed window W_{out}. The following steps are used.

1. First, given the size of the seed, $(A \times B)$ with $N = \max(A, B)$, we want to segment the seed from the background of the prostate fluoroscopy. Define an inner window size $N \times N$ and the outer enclosed window size $M \times M$, where $M > N$. Figure 2 shows the inner widow size 5×5 (W_{in}), the outer enclosed window size 11×11 (W_{out}) and the center pixel $C(i,j)$.

2. Next, considering the pixels in the inner window, we define a set of rotating segment lines starting from the center pixel to the edge of the inner window. The maximum separation between the segment at the inner window boundary is three pixels and the minimum separation between the segment at the inner window boundary is one pixel. These ranges will increase the number of segments when the inner window is large and reduce the number of segments when the inner window is small. Since the seeds are cylindrical in shapes, by using these rotating segments, we only process objects that are of interest in lieu of the entire inner window's pixels. Figures 3(a) to 3(h) show examples of the orientation of these segments. One of these rotated line segments best represents the intersection between the seed (or seeds in case of overlapping seeds) that we are trying to segment.[1]
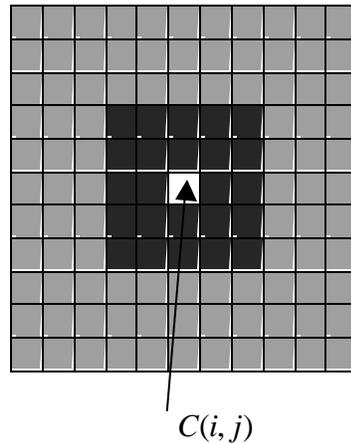

$C(i, j)$

Figure 2. Inner and outer windows of the spoke algorithm.

3. After the rotated segments are defined, we compute the mean intensity pixel value of the pixels that fall on each segment to create the inner line segment nodes, L_n. From Fig. 3(a) to 3(h), we compute these inner segment nodes as:

$$L_0^o (i, j) = \frac{1}{l}\sum_{p=0}^{l-1} I(W_{i, (j+p)}), \qquad L_{180}^o (i, j) = \frac{1}{l}\sum_{p=0}^{l-1} I(W_{i, (j-p)});$$

$$L_{45}^o (i, j) = \frac{1}{l}\sum_{p=0}^{l-1} I(W_{(i-p), (j+p)}); \qquad L_{225}^o (i, j) = \frac{1}{l}\sum_{p=0}^{l-1} I(W_{(i+p), (j-p)});$$

$$L_{90}^o (i, j) = \frac{1}{l}\sum_{p=0}^{l-1} I(W_{(i-p), j}); \qquad L_{270}^o (i, j) = \frac{1}{l}\sum_{p=0}^{l-1} I(W_{(i+p), j});$$

$$L_{135}^o (i, j) = \frac{1}{l}\sum_{p=0}^{l-1} I(W_{(i-p), (j-p)}); \qquad L_{315}^o (i, j) = \frac{1}{l}\sum_{p=0}^{l-1} I(W_{(i+p), (j+p)}).$$

---

[1] The spoke algorithm can be generalized to segment different shape objects by defining specific rotating segment characteristics. For example, to segment circularly shaped objects, a rotating triangular shape can be used instead of the rotating line to look for cylindrical objects.

where (i, j) is the coordinate of the center pixel of the inner window and l is the total number of pixels in the segment.
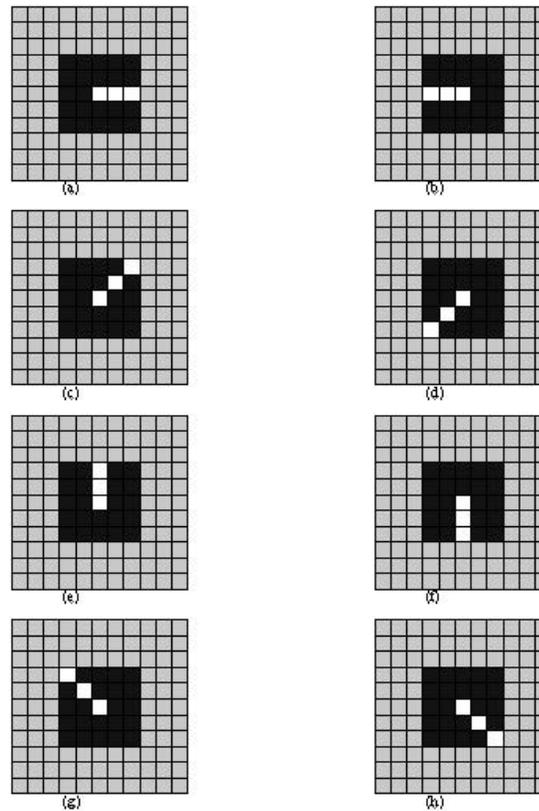

Figure 3. Orientation of spoke segments.

4. To further enhance our detection, we assign to the inside node, N_i, the mean intensity pixel value of the inside window, W_{in}. The inside node gives an indication of the background level of the region immediately surrounding the seeds. It can be described as follows:

$$N_i = \frac{1}{N^2} \sum_i \sum_j I(W_{in}).$$

5. In addition to the inside nodes, N_i, the local pixels surrounding the seed will be used to further enhance the detection decision. These pixels are from the outside of the window W_{in} and the pixels inside of the window W_{out}. This region can be represented as $W_{ext} = W_{out} - W_{in}$ with $(M^2 - N^2)$ pixels.

6. Finally, we define an outside node, N_o, the mean intensity pixel value of W_{ext} region. It can be expressed as follows:

$$N_o = \frac{1}{M^2 - N^2} \sum_i \sum_j I(W_{\text{ext}}).$$

In some high contrast areas of the image, the inner nodes detected these changes and consider these areas as potential seed areas. The outside node provides an isolated region not being segmented and represents non-seed area to remove false detection for large areas that inner nodes, Ln, detected.

Our goal is to determine if there is a seed or seeds in one of these nodes. In order to evaluate the likelihood that one or more of these nodes contain the seeds in the inner window, the probability of a segment node that contains a seed can be represented as

$$P(L_n \mid N_i \, N_o) = P(L_n \, N_i \, N_o) \, / \, P(N_i \, N_o).$$

From the line segment nodes, L_n, we select the node with the largest mean intensity pixel value and use this value for future computation of the highest probability that the node contains the seed. It is expected that optimal detection will occur when the ratio of probability of finding the seed in the inner nodes, N_i, to that in the external nodes, N_o, is maximized.

4. SPOKE TRANSFORM

The spoke transform involves the convolution of the original image with the spoke kernel as described above. The spoke transform will produce a new value for each pixel. By using these inner line segments and creating inner nodes, these nodes use different intensity values based on the inner window for different areas of the image. The transformation is given by:

$$S(i, j) = \sum_k \sum_l (S_1(i - k, j - l) + S_2(i - k, j - l)),$$

Where
$$S_1(i, j) = \begin{cases} \text{Max}(L_n) - N_i & C(i, j) > N_i \text{ and } N_i > N_o. \\ 0 & \text{Otherwise.} \end{cases}$$

$$S_2(i, j) = \begin{cases} \text{Max}(L_n) & \text{Max}(L_n) > N_i \text{ and } N_i > N_o. \\ \text{Min}(L_n, C(i, j)) & \text{Otherwise.} \end{cases}$$

The S_1 transformation enhances the differences of the pixel intensity values between the seeds and its surroundings. The S_2 transformation enhances the contrast of the seeds by suppressing intensity value of its surrounding pixels. This second transformation provides the compensation mechanism for the hidden seeds in the images. The output of the $S(i, j)$ process will produce a contrast enhanced images of the original image. From the S_1 transformation image, a global histogram is used to determine the threshold to segment the image and similarly for the S_2 transformation image. The threshold is determined beginning with the mean of the histogram and manually varying the threshold to achieve the best segmentation. The combination of the two thresholded images gives the final segmented seeds.

5. RESULTS AND DISCUSSION

Figure 4 shows an original palladium-103 (Pd-103) seed image. Figure 5 zooms in on the seed area. The seed size, approximately 5×3 pixels, is typical for C-arm fluoro images. Since the seeds' intensities vary over a wide range and the backgrounds also have similar ranges, the spoke transform is useful for segmenting the seeds. Figure 6 shows the S_1 transformation and Fig. 7 shows the result of segmented image with $W_{in} = 5 \times 5$ and $W_{out} = 11 \times 11$. Figure 8 shows the S_2 transformation and Fig. 9 shows the result of segmented image with $W_{in} = 5 \times 5$ and $W_{out} = 11 \times 11$. Figure 10 shows the final result of the segmentation after combining S_1 and S_2 transformation results and using morphological processing to remove large areas in the bottom right corner. We also applied our method to another type of seed. Figure 11 shows the original image of an iodine-125 (I-125) seed. The image was captured on film and subsequently digitized with a laser film scanner. The average size of the seed is 14×5 pixels. Figure 12 shows the S_1 transformation and Fig. 13 shows the S_2 transformation with $W_{in} = 7 \times 7$ and $W_{out} = 14 \times 14$. Figure 14 shows the final result of the segmentation.

The spoke transform greatly facilitated the seed segmentation process by enhancing and isolating the seeds from the background. It also eliminates many fault edges that the traditional edge detection methods. However, the spoke method is not yet fully automated. The step that requires manual intervention is the gray scale thresholding after application of *spoke transform*. The global histogram based thresholding technique was not always reliable in the high intensity pixel value areas.

Segmentation of the small seed is related to the problem of determining the edge. The *sticks transform*[12] has been used in determining the edges of the prostate in ultra-sound images. The spoke transform segments have the similar function as the stick transform method. The stick line segment is designed to determine the most likely to be the edge while the spoke segment is designed to determine the most likely to be the seed. Both methods select the best of the rotating segments as a possible solution but the spoke transform also utilizes the two concentric windows to further enhance the detection. The stick line segment is centered at the central pixel while the rotating segment only uses center pixel as a pivoting point. This provides us more precision in determining the end seeds when compare to the central pixel.

6. CONCLUSION

We have presented a new approach to segment the radioactive seeds in prostate x-ray images. The method uses different kernel windows for different backgrounds and seeds. These nodes use different scales based on the inner window for different areas of the image. This method also effectively utilizes and compares the seeds and its surrounding regions. The algorithm demonstrates the ability of the spoke transform to segment hidden seeds in both Pd-103 and I-125 images.
Future work is proposed for automating the thresholding process.

REFERENCES

1. S.T. Lam, R.J. Marks II, P. Cho, "Prostate boundary detection and visualization in TRUS Images", International Conference on the Use of Computers in Radiation Therapy XIII, Heidleberg, Germany, May, 2000, pp. 99-101.

2.   H. Suzuki; N. Inaoka; M. Mori; H. Takabatake; A. Suzuki, "Segmentation and analysis of pulmonary blood vessel from X-ray CT images", Engineering in Medicine and Biology Society, 1988., Proceedings of the Annual International Conference of the IEEE, 1988, pp. 404 -405 vol. 1.

3.   M. Ruben; G. Mireille; J. Diego; C. Carlos; T. Javier, "Segmentation of ventricular angiographic images using fuzzy clustering", Engineering in Medicine and Biology Society, 1995., IEEE 17th Annual Conference, 1997, pp. 405 -406 vol. 1.

4.   V.V. Vinod; S. Chaudhury; J. Mukherjee; S. Ghose, "A connectionist approach for gray level image segmentation", Pattern Recognition, 1992. Vol.III. Conference C: Image, Speech and Signal Analysis, Proceedings., 11th IAPR International Conference on, 1992, pp. 489 –492

5.   P. Cho and B. Adams, "Automated seed recognition for intraoperative prostate brachytherapy dosimetry", Med. Phys. 26, 1999, pp. 1146.

6.   A. Houston, S. Premkumar, D. Pitts, "Prostate ultrasound image analysis: localization of cancer lesions to assist biopsy". Eighth IEEE Symposium on Computer-Based Medical Systems, 1995, pp. 94-101.

7.   J. C. Russ, The Image Processing Handbook, CRC Press, Boca Raton, 1992.

8.   L. Shen, Y. Shen, R. Rangayyan, "Shape characterization and its applications", 1994 International Symposium on Speech, Image Processing and Neural Networks, 1994, pp. 9-12.

9.   M. Salotti and C. Garbay, "A new paradigm for segmentation", Pattern Recognition, 1992, Conference C: Image, Speech and Signal Analysis, pp. 611-614, vol 3.

10. B. Cramariuc, M. Gabbouj, J. Astola, "Clustering based region growing algorithm for color image segmentation", Digital Signal Processing Proceedings, 1997, 13th International Conference, pp. 857-860, vol 2.

11. Y. Yu, J. Wang, "Image segmentation based on region growing and edge detection", Systems, Man, and Cybernetics, IEEE SMC '99 Conference Proceedings. 1999, pp. 798-803, vol. 6.

12. S. D. Pathak, R. G. Aarnink, J. J. de la Rosette, V. Cha-lana, H. Wijkstra, F. M. J. Debruyne, and Y. Kim, "Quantitative three-dimensional trans-rectal ultrasound for prostate imaging", Proceedings, SPIE Medical Imaging, 1998, pp 83-92.
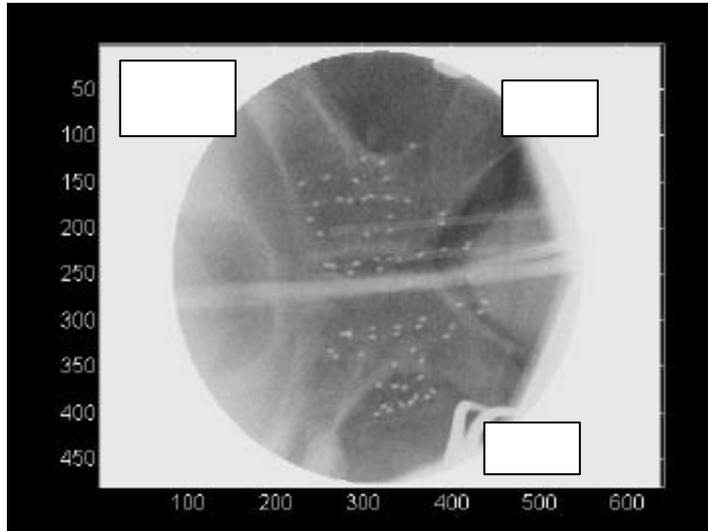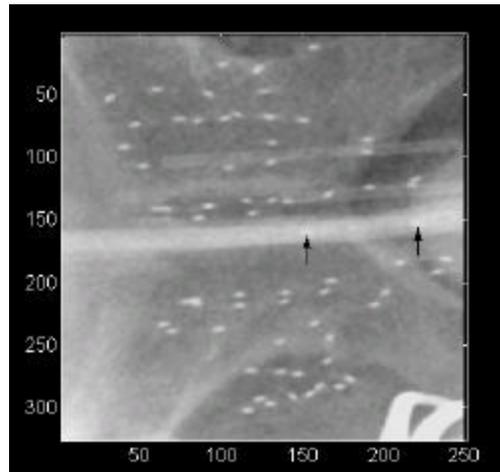
Figure 4. Original Pd-103 image.

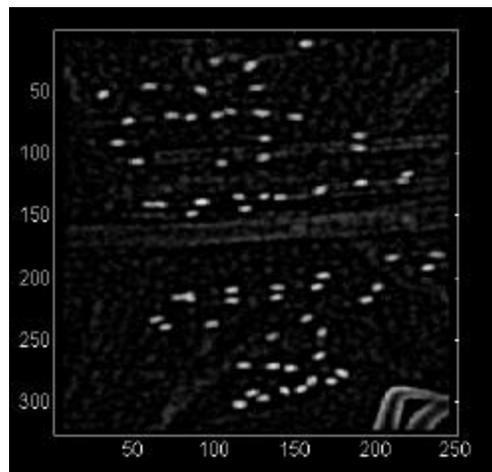Figure 5. Seeds area (Arrow indicates hidden seeds).
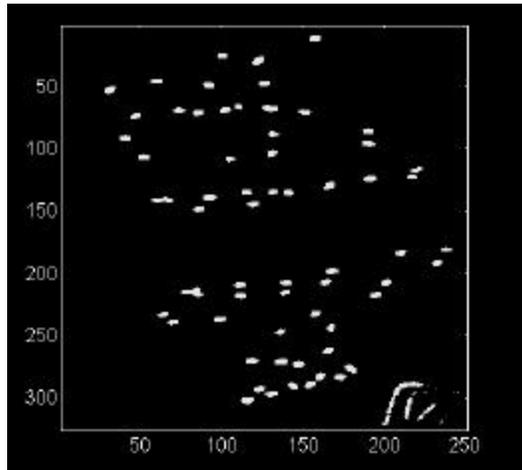

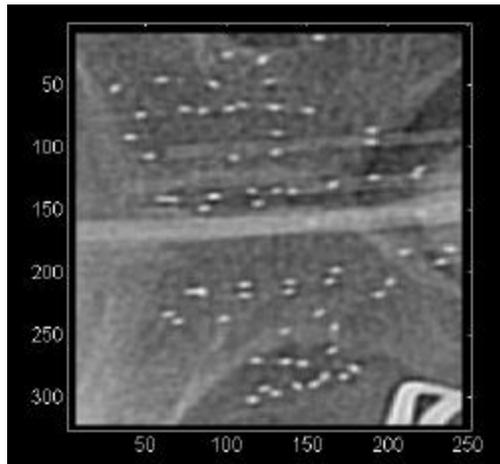Figure 6. Result of S_1.

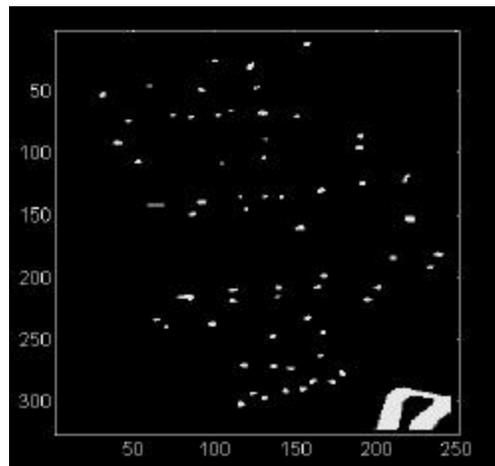Figure 7. Segmentation of S_1.

Figure 8. Result of S_2.

Figure 9. Segmentation of S_2.

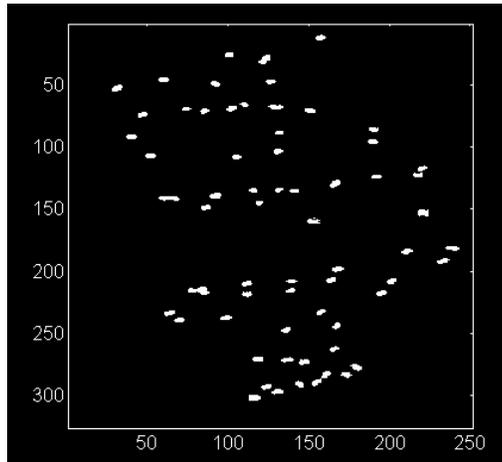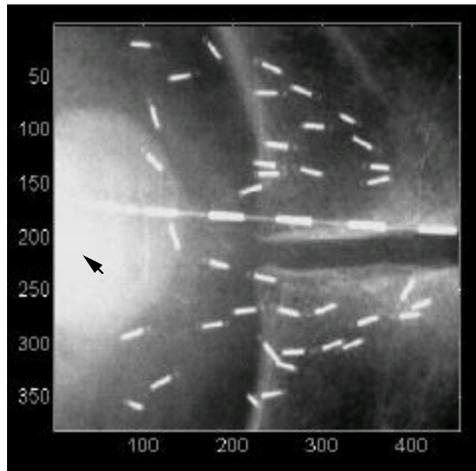Figure 10. Final segmentation result.

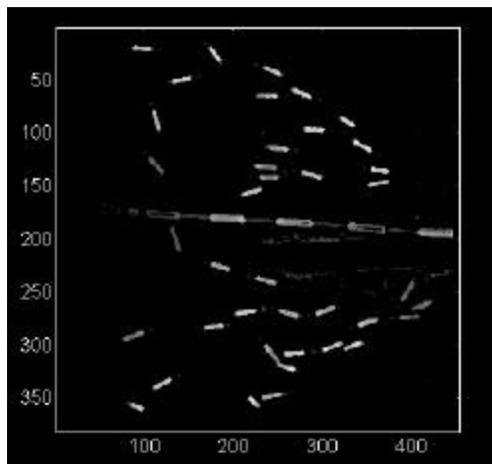Figure 11. Original I-125 image (Arrow indicates hidden seed).
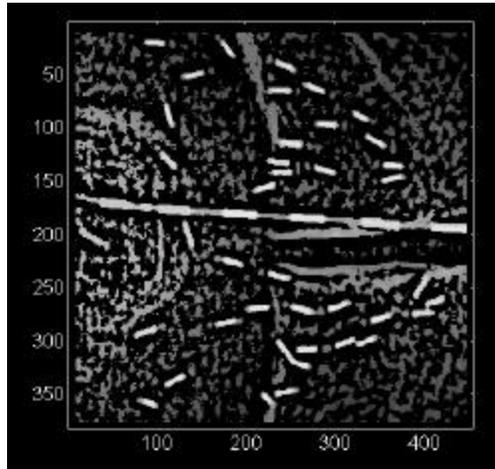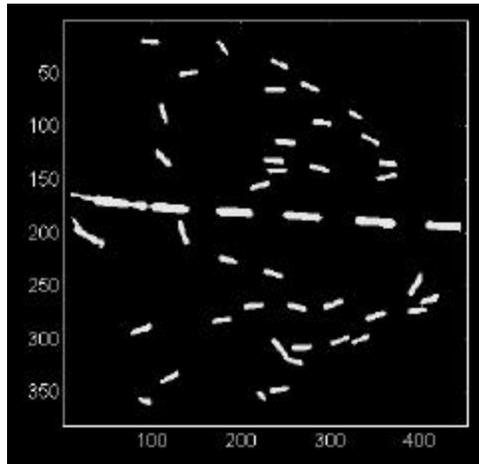

Figure 12. Result of S_1.

Figure 13. Result of S_2.

Figure 14. Final segmentation result.